JOURNAL OF BONE AND MINERAL RESEARCH
Volume 17, Number 5, 2002

Cell Proliferation and Apoptosis During Fracture Healing

GANG LI, GRAINNE WHITE, CHRIS CONNOLLY, and DAVID MARSH

ABSTRACT

This study investigated the relation between cell proliferation and apoptosis during fracture healing in a mouse femoral fracture model. Left femoral osteotomies were performed in 30 mature male CFLP mice immobilized with uniplanar external fixators. Six animals were killed on days 2, 4, 8, 16, and 24 postfracture for examination. Localization of cell proliferation was examined using immunohistochemistry with proliferating cell nuclear antigen (PCNA) monoclonal antibody. Apoptotic cells were visualized with the terminal deoxynucleotidyl transferase (TdT)–mediated deoxyuridine triphosphate (dUTP)-biotin nick end-labeling (TUNEL) method. Images of each time-specific specimen were captured. The total callus area, the positively labeled cells by PCNA, and TUNEL per high-power field were quantified. Cell proliferation and apoptosis were found coexisting during the entire period of study. In the early phases of fracture healing (days 2–8), PCNA-positive labeling was predominant and peaked at day 8 and the TUNEL-positive labeling was minimal. In later stages of fracture healing (days 16–24), PCNA expression declined at day 16 as callus ossification and remodeling spread within the fracture site and apoptosis was the dominant cell activity with the TUNEL-positive labeling peaking at day 16 and declining sharply at day 24. These cell activities were reflected by the change of fracture callus, where there was a continuous increase in total callus area to day 16 and subsequent decrease at day 24. This study indicated that cell proliferation and apoptosis are coupled events during fracture repair, cell proliferation is active at the early stages, and apoptosis is active during the phase of callus remodeling. (J Bone Miner Res 2002;17:791–799)

Key words: fracture healing, cell proliferation, apoptosis, terminal deoxynucleotidyl transferase–mediated deoxyuridine triphosphate-biotin nick end-labeling, proliferating cell nuclear antigen, mouse

INTRODUCTION

FRACTURE REPAIR is a complex physiological process during which bone shows a remarkable ability to mount a repair process that not only restores the mechanical integrity but also anatomical configuration. After the initial bony union, there is a prolonged phase of callus remodeling to restore the anatomical configuration of the bone. It has become widely recognized that many of the cellular and biochemical processes that occur during fracture healing correspond to those that take place during skeletal development.[1–3] Our current knowledge suggests that the genetic mechanisms that regulate fetal skeletogenesis also regulate adult skeletal regeneration, pointing to the important regulators of angiogenesis and ossification in bone regeneration.[3–5]

Cell proliferation plays an important role in both physiological and pathological activity. In all regenerating tissue, the initial commitment of a stem cell progeny is followed by amplification.[6] In recent studies, Iwaki et al.[7] have localized and quantified the proliferating cells in each of the cellular events that occur during fracture repair. The work of Lee and coworkers[8] was in agreement with the findings of Iwaki et al.[7] and suggested that proliferating mesenchymal

The authors have no conflict of interest.

Trauma Research Group, Department of Trauma and Orthopedic Surgery, Queen's University of Belfast, Musgrave Park Hospital, Belfast, United Kingdom.

cells play a key role during the fracture healing process. The distribution of proliferating cells and the degree of cell proliferation vary according to the period after the fracture, suggesting the existence of local regulatory factors such as growth factors and cytokines.[9,10]

Maintenance of adult tissue mass, organogenesis, and normal tissue remodeling are determined by a combination of cell proliferation, cell differentiation, and cell programmed death.[11–16] Apoptosis is a genetically determined, programmed, and physiological mode of cell death, characterized by specific morphological, biochemical, and molecular changes.[17] The suggestion that cell death has an active function in biological tissues has raised the fundamental question of how "death" can have a positive role in life; "today, however, from a biological view, cell death appears to be one of life's undissociable companions."[18]

For years the regulation of cell number has been considered mainly in terms of cell proliferation; however, the recent investigations into apoptosis would suggest that it is equally important.[19–21] The dependence on the surrounding microenvironment confirms that cell death is a fundamental property of cells, where unwanted cells are eliminated quickly and neatly. The importance of such controls in multicellular organisms can be seen during wound healing in which misplaced cells and/or excess cells are eliminated rapidly.[22] Likewise, the existence of such controlling factors regarding cell proliferation and cell death is evident in the proliferating tissues, found in embryonic development,[23] cancer,[24] and bone repair.[8,19,25] The aim of this study was to investigate the timely and spatial relationship of cell proliferation and programmed cell death (apoptosis) events during fracture repair in a mouse femoral fracture model.

MATERIALS AND METHODS

Animal model

All animal experimental procedures were approved and performed under the control of the guidelines for the Animals (Scientific Procedures) Act 1986, British Home Office. Thirty skeletally mature (35–45 g) male CFLP mice (Harlan, Oxford, UK) were used. General anesthesia for all operative procedures was achieved by administration of 2% isoflurane, 49% nitrous oxide, and 49% oxygen via a Hunt mask with a scavenging system. One milliliter of 5% dextrose was administered subcutaneously at induction of anesthesia for fluid maintenance during the operative procedure.

The mouse femoral fracture model was adapted from Connolly et al.[26] In brief, mice under general anesthesia and aseptic conditions had a lateral incision through shaved skin and fascia lata from the left knee to the greater trochanter. The plane between the vasti and hamstrings was opened by blunt dissection to expose the femur. Four bicortical pinholes were drilled and a low-energy middiaphyseal osteotomy of the femur was performed. A custom-made drilling jig and hand saw were used ensuring exact centralization of the transverse osteotomy between the inner two pinholes. Four-pin, unilateral, single-plane, mini external fixators were applied, stabilizing the fracture. Fascia lata and skin were closed with polyglactin absorbable sutures.

Sample preparation

Six mice were killed at 2, 4, 8, 16, and 24 days postfracture. The left femur was excised by sharp dissection disarticulation through the knee and hip joints with the external fixator and soft tissues in situ. Two orthogonal oblique radiographs were taken of each specimen. After excision of the femur from the killed animals, all specimens were coded and fixed in 10% buffered formalin, pH 7.0, for 24 h. The tissues were rinsed in distilled water before being transferred into the decalcifying solution. The specimens were decalcified in 8% EDTA (pH 7.0–7.5; Sigma Chemical Co., Poole, UK) for 3 weeks. EDTA was changed each week. On completion of decalcification of the tissues, the external fixators were removed carefully and the specimens were embedded in paraffin wax. Five-micrometer-thick sections were cut in approximately the central coronal plane of the samples using a rotary microtome (Microm HM315; Microm, Walldorf, Germany) and the sections were placed on the poly-L-lysine–coated slides (Sigma Chemical Co.) and heated at 60°C for 15 minutes and then stored in a clean box before use.

Histological and immunostaining examination

The sections were stained routinely with the standard histological staining method, hematoxylin (Gill's no. 3) and 0.5% eosin (Sigma Chemical Co.).

For immunohistochemistry, 5-μm-thick sections were deparaffinized in xylene and immersed in graded ethanol and distilled water. Endogenous peroxidase activity was inhibited by immersing the tissue sections in 0.3% hydrogen peroxidase for 20 minutes at room temperature. Subsequently, the sections were rinsed in phosphate-buffered saline (PBS). To facilitate antibody binding, sections were incubated for 30 minutes at room temperature with proteinase K solution (20 μg/ml; DAKO, Dorset, UK) to unmask the antigen binding sites. Then, the sections were incubated with purified rabbit anti-mouse proliferating cell nuclear antigen (PCNA) monoclonal antibody (1:100 ratio in PBS; DAKO) for 45 minutes at room temperature. Subsequently, the primary antibody was blotted and the tissues were rinsed with PBS. The secondary purified goat anti-rabbit/mouse biotinylated antibody (1:100 in PBS; DAKO) was applied to the sections and incubated for 30 minutes at room temperature. Sections were rinsed in PBS and then incubated with streptavidin-peroxidase (1:50 in PBS; DAKO) for 30 minutes at room temperature. Diaminobenzidine Chromagen solution (0.5 mg/ml of 2,4,2′,4′-tetrabiphenyl hydrochloride; Sigma Chemical Co.) in 0.1 m of imidazole in PBS, containing 0.3% hydrogen peroxidase, was added to the sections and incubated at room temperature for 5 minutes. After a brief rinse in distilled water, the tissue sections were counterstained in Gill's no. 3 hematoxylin (Sigma Chemical Co.) at a dilution of 1:3 for 5 minutes, rinsed in distilled water, and dehydrated through a series of graded ethanol solutions to xylene, mounted in DPX, and examined by light microscopy.

Primary antibody was omitted as a negative control for the immunostaining method. The small intestine is a high-proliferating tissue and was used as a positive control for the detection of proliferating cells. Nerve tissue, a low-proliferating tissue type, was used as a negative control for the PCNA immunostaining.

DNA nick end-labeling (terminal deoxynucleotidyl transferase–mediated deoxyuridine triphosphate-biotin nick end-labeling)

The method of terminal deoxynucleotidyl transferase (TdT)–mediated deoxyuridine triphosphate (dUTP)-biotin nick end-labeling (TUNEL) was first described by Modak and Bollum[27] and further modified by Gavrieli et al.[28] In this study, TUNEL staining was used as an indicator of apoptosis. The TUNEL method is a highly sensitive assay, which allows the detection of apoptosis at the single-cell level. The method used in this study is based on the specific binding of TdT to 3′-OH ends of DNA fragments. TdT has the capacity of adding nucleotides to the free 3′ ends and thus tailing the nicks with the fluorescein-labeled oligonucleotide dUTP. The signal is detected by antibody to fluorescein, enabling conventional histochemical identification of programmed cell death by light microscopy.

An in situ cell death detection kit (Roch Molecular Biochemicals Co., East Sussex, UK) was used for the detection of apoptosis. In brief, sections were deparaffinized by immersion in xylene and through a graded series of ethanols. After washing in Tris-buffered solution (TBS), sections were permeabilized using 0.1% Triton-X 100 for 20 minutes. The sections were washed for 5 minutes in TBS before labeling with the TUNEL reaction mixture for 45 minutes according to the manufacturer's instructions, where optimal amounts of fluorescein-labeled dUTP and TdT were used. The reaction was terminated by immersing the slides in TBS and rinsed. To detect the whereabouts of the fluorescein-labeled dUTP, the slides then were incubated with sheep antifluorescein antibody conjugated with alkaline phosphatase (ALP) for 30 minutes (Roche Molecular Biochemical Co.). After rinsing in TBS, the slides were developed with either substrate solution containing TBS, Fast red TR, and naphthol AS-MX (red stain) or BCIP/4-nitro blue tetrazolium (NBT) substrate (blue stain; Sigma Chemical Co.). Finally, the slides were mounted in glycine jelly (Sigma Chemical Co.) and analyzed by light microscopy.

For a negative control, slides were incubated with a solution containing only nucleotide mixture in reaction buffer, without TdT. In addition, rabbit peripheral nerve tissue, a tissue having a low cell turnover, was adopted as a real negative control, and the same nerve tissue section pretreated with DNAse I (20 mg/ml; Sigma Chemical Co.) was used as a methodological positive control.

Image analysis

All coded sections of the specimens were analyzed blindly. Each of these images was viewed by light microscopy (Leica DMLB; Leica Microscopy Systems, Ltd., Heerbrugg, Switzerland) under 50× magnification. A digital image of each section was grabbed onto a Kontron Vidas Image Analyser (Kontron KMBH, Munich, Germany). The mean femoral diameter, medial, intramedullary, and lateral areas of woven bone, cartilage, and fibrous tissues were calculated in pixels. The measurement was done manually by tracing around the respective areas on screen with a mouse. The femoral diameter was calculated as the mean of four transverse measurements taken at the proximal and distal edges of the inner pinholes on each section of the specimen. This data were transferred electronically to a statistical spreadsheet (version 9; SPSS, Inc., Chicago, IL, USA) eliminating clerical errors. All areas were normalized against the mean femoral diameter on the respective section and expressed as a ration of pixels to standardize the area variations created by the range of animal sizes.

For quantifying the PCNA immunostaining and the TUNEL-labeling results, the sections were analyzed under a Leica research microscope (Leica DMLB; Leica Microscopy Systems, Ltd.). A validated method of quantifying immunostaining results was adapted.[29] In brief, under 100× magnification, the area (3 mm^2) containing the maximum number of the positively labeled cells by PCNA or TUNEL was chosen in five defined regions near the fracture site, namely, the fracture gap and two subregions distal and proximal to the fracture gap on both sides of the fractured cortices. Three random images of 0.75 mm^2 from each selected area (3 mm^2) were then taken under high magnification (×400). All the images of each specimen were captured via a digital camera (Eastman Kodak Co. DS120; Eastman Kodak Co.Rochester, USA) and saved as JPEG files. The images were opened in Scion Image Software (Scion Corp., Frederick, MD, USA); the number of the positively labeled cells in each image was counted by two independent observers, and the mean of the two was calculated. Mean numbers of positively labeled cells per high-power field (0.75 mm^2) for PCNA and TUNEL from the five regions of each specimen section then were calculated and used for further statistical analysis. Next, the overall mean numbers of positively labeled cells per high-power field for PCNA and TUNEL of each time point were obtained and plotted and data were expressed as mean ± SE.

Statistical analysis

The calculated means of the normalized total callus area (the numbers of positively labeled cells of each type at each specific time point) were first tested by one way analysis of variance (ANOVA) with the factor "time," to identify significant differences between the groups. If a significant difference was found, pairwise comparisons were performed using Student's *t*-test. If $p \leq 0.05$, it was considered significant. All statistical analyses were carried out using a commercially available statistical program by SPSS, Inc. (version 9).

RESULTS

Histological and histomorphometry examination

Hematoma formation occurred initially as seen on day 2 postfracture. Invasion by fibrovascular tissues converted the

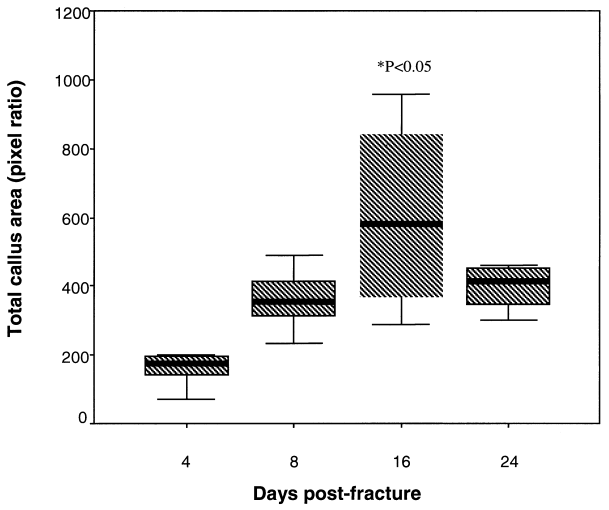

FIG. 1. Box plot showing the histomorphometric measurement results of the fracture callus. There was a continuous increase in total callus area to day 16 and subsequent decrease on day 24 (*$p < 0.05$, Student's *t*-test; means and SEs were plotted).

hematoma into a mixture of bone, cartilage, and fibrous tissues, which were seen throughout days 4–8 postfracture. Callus formation began with proliferation and differentiation of mesenchymal cells on day 4; new bone formation was evident at this point. Cartilage tissue appeared in and around the fracture site starting on day 8 postfracture. Intramembranous ossification was evident under the periosteum at 8–16 days postfracture together with endochondral ossification. As the collagen fibers and matrix were laid down, they became mineralized to form woven bone, appearing first on day 4 and becoming the predominant tissue type on day 16. The characteristic nonlamellar structure of woven bone could be seen on day 8 and day 16 with the presence of randomly orientated crisscross fibers. A bony sleeve was evident on day 16 and day 24 postfracture, enclosing the fracture site.

Histomorphometric analysis of 24 specimens (excluding six specimens from day 2 postfracture) indicated that the total callus area increased to a maximum at day 16 and subsequently reduced on day 24 postfracture (Fig. 1). After day 16, the amount of fibrous tissue and cartilage in the fracture callus fell sharply. A marked rise in the amount of new bone, as a proportion of the total callus area, was noted on day 24 postfracture, and this was mirrored by a fall in fibrous tissue and cartilage area, with a fall of total callus area on day 24 compared with day 16 postfracture (Fig. 1).

Detection of cell proliferation (PCNA) by light microscopy

No negligible PCNA labeling was observed in any of the negative controls under the experimental conditions used in this study (Fig. 2A). For positive controls in the small intestine, PCNA showed intense labeling as expected (Fig. 2B).

Proliferation of undifferentiated mesenchymal cells was evident in the initial stages first in the periosteum and tissue immediately around the fracture gap (Fig. 2C) and extending throughout the whole length of the bone along the periosteal surfaces. There were proliferative cells found on the surfaces of the periosteal callus on day 4 (Fig. 2D). A rise in cell proliferation was evident on day 8, PCNA-positive chondrocytes (Fig. 2E) were seen adjacent to the fracture site, and there was a thickening of the periosteum with extensive PCNA-positive labeling (Fig. 2F). Cell proliferation continued as the cartilage became concentrated between the fractured ends and eventually was replaced by woven bone (Fig. 2G). The decline in cell proliferation from day 8 to 16 was significant, at which point the main tissue type was woven bone (Fig. 2H), with a drop in mean PCNA-positive cells per high-power field, from 47.40 ± 8.60 (day 8) to 32.0 ± 7.65 (day 16). At day 24, a majority of the PCNA-positive cells were seen in the remaining cartilage and on the woven bone surfaces (Fig. 2I) as the bone remodeling began. A significant decline in PCNA-positive cells was evident between day 16 and 24, as the mean PCNA-positive cells per high-power field dropped to 9.80 ± 1.97 (day 24).

Statistically, there is a significant difference in cell proliferation over time at the 5% level. No significant difference was evident between the day 2 and 4, postfracture ($p = 0.265$, *t*-test). A statistically significant difference (increase) was found between day 4 and day 8, postfracture ($p = 0.037$, *t*-test). Statistically, day 16, in comparison with day 8, indicated a significant decrease of the PCNA positive labeling index ($p = 0.02$, Student's *t*-test). Likewise, there was a significant decrease between day 16 and 24 ($p = 0.013$, Student's *t*-test).

Detection of cell death (TUNEL) by light microscopy

The nerve tissue negative control showed no or minimal TUNEL staining (Fig. 3A). Extensive numbers of TUNEL-positive cells (in dark blue when BCIP/NBT substrate was used) were seen in the tissue sections treated with DNAse I as methodological positive control (Fig. 3B).

TUNEL-labeled cells showed a loss of cell contact, shrinking away from neighboring cells, leading to the formation of halos around the cell bodies. Nuclear and cytoplasmic condensation caused apoptotic cells to obtain a more spheroidal morphology and rounded appearance. Some positive TUNEL-labeled cells (pink/red when the Fast red TR and naphthol AS-MX substrate were used) were seen in the periosteum and the newly formed periosteal callus near the fracture gap at the early stages of fracture healing (days 2–4; Figs. 3C and 3D), followed by a slight increase in TUNEL labeling in chondrocytes and osteoblastic cells in the callus on day 8 postfracture (Fig. 3E). The number of the TUNEL-labeled cells in the newly formed callus and cartilage peaked on day 16 postfracture (Figs. 3F and 3G) and significantly declined on day 24, where the TUNEL-labeled cells were mainly seen in the remaining cartilage islands (Fig. 3H) and in the newly remodeled lamellar bone (Fig. 3I). In the early stages of healing, TUNEL-labeled cells per high-power field were low with a

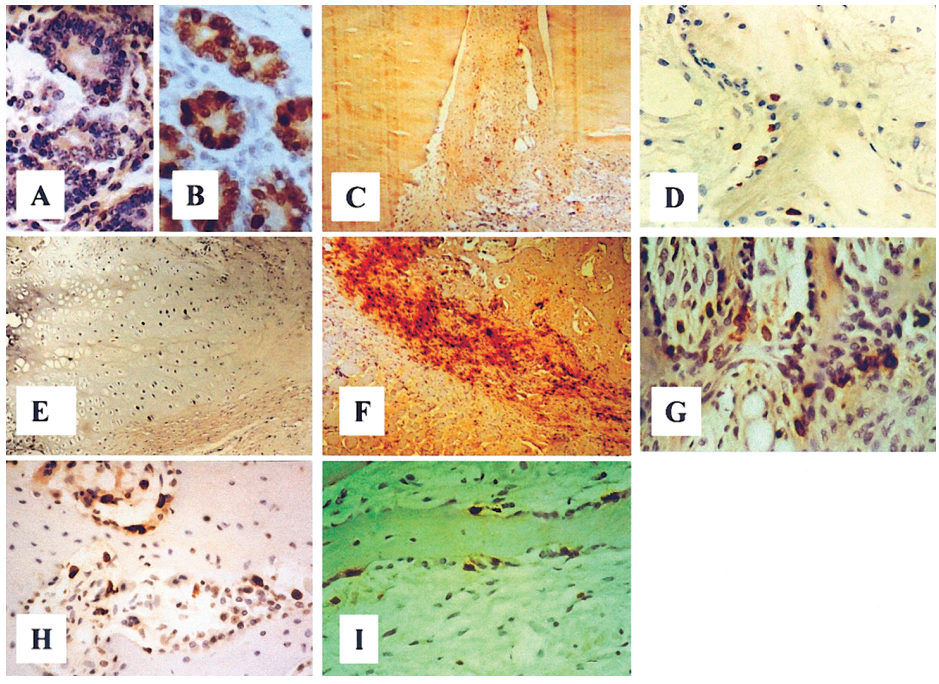

FIG. 2. Representatives of immunostaining results of PCNA antibody. (A) Negative control (without primary antibody) on mouse small intestine. (B) Positive control of PCNA immunostaining on the mouse small intestine. (C) Proliferation of undifferentiated mesenchymal cells (brown) was evident on day 2 in the fibrous tissues in the fracture gap. (D) On day 4, a few PCNA-positive cells (brown) were seen at the surfaces of the periosteal callus. (E–G) A rise in cell proliferation was evident on day 8; PCNA-positive cells (brown) were seen (E) in the cartilage region near fracture gap, (F) in the periosteum region adjacent to fracture gap, (G) and in the newly formed periosteal callus. (H) On day 16, cell proliferation declined as the cartilage became concentrated between the fractured ends and eventually was replaced by woven bone; PCNA-positive cells (brown) were seen mainly at the surfaces of the newly formed woven bone. (I) On day 24, PCNA-positive cells (brown) were sparse in both the remaining cartilage and the surfaces of the newly formed bone (panels A–E were counterstained with hematoxylin; original magnification for panels A, B, D, G, H, and I, ×400, and panels C, E, and F, ×100).

mean of 11.40 ± 1.03 on day 2 and 14.60 ± 4.65 on day 4. The mean TUNEL-labeled cells increased to 27.20 ± 5.35 on day 8 and peaked at 47.60 ± 2.50 on day 16. TUNEL-labeled cells were found in the fibrous tissues in the fracture gap on day 2 and day 4, cartilage tissues were found on day 8 and day 16, and new osteoid tissue (woven and lamellar bone) appeared on days 8–24 postfracture. A decline in the mean number of the TUNEL-labeled cells per high-power field on day 24 (16.80 ± 4.31) was evident mainly in the newly formed bone tissues.

As shown in Fig. 4, ANOVA test found a significant difference in the numbers of the TUNEL-labeled cells between the time points after fracture. Further paired tests showed that no significant difference was found in the number of TUNEL-labeled cells per high-power field between day 2 and day 4 groups ($p > 0.05$, Student's *t*-test). A significant difference (increase) was found between the day 4 and day 8 postfracture groups ($p = 0.013$, Student's *t*-test). Testing of day 8 and day 16 groups established a significant increase in the number of TUNEL-labeled cells ($p = 0.004$, Student's *t*-test). A significant decrease in the number of TUNEL-labeled cells was found between day 16 and day 24 groups ($p = 0.001$, Student's *t*-test).

A summary of cell proliferation and apoptosis activities after fracture at different histological regions of the fracture gaps is given in Table 1.

DISCUSSION

The mouse femoral fracture model with external fixator used in this study provided an excellent experimental system to study cellular events such as proliferation and apoptosis during fracture repair. This model also can be used to study the role of apoptosis in fracture healing in transgenic mutants. Although there were many previous studies on cell proliferation and apoptosis during fracture healing, the reports were scattered. This study was designed specially to further characterize the apoptosis occurring together with cell proliferation at different time points during fracture repair in a controlled animal experimental system.

Localization of cell proliferation was examined using immunohistochemistry with PCNA monoclonal antibody, which has been used and reported previously.[7,30] Cell proliferation appears to be a major cellular response at the beginning of each cellular event (inflammation, chondrogenesis, intramembranous, and endochondral ossification), concurring with Iwaki et al.,[7] who concluded that fracture healing begins with cell proliferation. Thickening of the periosteum and positive PCNA labeling of the periosteum in this study (Fig. 2F) suggest that the periosteum functions in mediating the initial cellular activities of fracture healing. Such findings are supported by Nakahara et al.[31] and Ozaki et al.,[32] who found that mesenchymal cells originated in

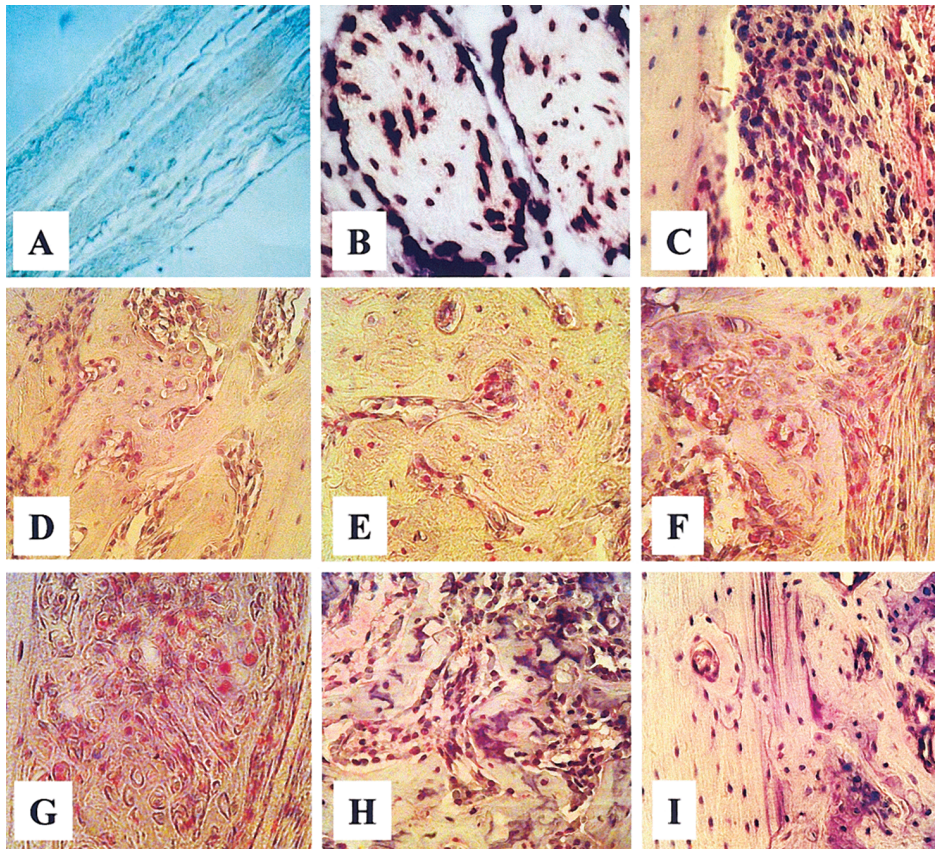

FIG. 3. Representatives of the TUNEL labeling results. (A) Negative control of TUNEL labeling on rabbit peripheral nerve tissue. TUNEL-labeled cells were rarely found. (B) When the nerve tissue was pretreated with DNAse I, extensive TUNEL labeling (dark blue) were seen. (C) Some positive TUNEL-labeled cells (pink) were seen on day 2 in the periosteum near the fracture gap. (D) On day 4, TUNEL-labeled cells (pink) were seen in the developing periosteal callus adjacent to the fracture site. (E) On day 8, more TUNEL-labeled cells (pink) were found in the newly formed callus. (F–G) On day 16, as endochondral ossification spread and intramembranous ossification occurred, extensive TUNEL labelings (pink cells) were found (F) at the surfaces of the newly formed callus and (G) in the cartilage region. (H and I) On day 24, as the newly formed (H) woven bone remodeled into (I) mature lamellar bone, the number of the TUNEL-labeled cells (pink) was significantly reduced (panels A and B, no counterstaining; panels C–I, counterstained with hematoxylin; original magnification, panel A, ×100, and panels B–I, ×400).

the periosteum, which appeared to be a source of cells necessary for osteogenesis and chondrogenesis during fracture repair. A significant level of cell proliferation, as revealed by PCNA labeling, appeared first in the undifferentiated mesenchymal cells and inflammatory cells at the fractured edges (days 2–4), followed by a peak in cell proliferation in primitive connective tissue and chondrocytes on day 8, and declined at later stages of fracture healing (days 16–24; Table 1). Results of this study are in accord with the proposed cell proliferation resulting from the inflammatory reaction and callus formation. As Tonna and Cronkite[33] reported, a decline in cell proliferation was evident when the chondroid callus was replaced with immature osseous tissue (endochondral ossification).

The TUNEL technique is sensitive enough to detect the few DNA-nicks accompanying the early stages of nuclear condensation and thus is useful in highlighting cells in the earliest stages of apoptosis. In this study, a morphological approach could not be relied on because of the difficulty in distinguishing between apoptosis and necrotic cell death at light microscopy level. Although TUNEL labeling is susceptible to both positive and negative artifacts,[34] there is no better alternative method for quantifying single-cell apoptosis in situ on histological sections at present. Transmission electron microscopy is the best approach to prove apoptotic changes qualitatively but is subjective and laborious and was not used in this study.

Apoptotic cells are so rapidly phagocytosed that identification and quantification of apoptosis have proven difficult; hence, the role of programmed cell death very often is underestimated. In this study, the number of TUNEL-positive cells in the callus areas was impressively high, suggesting that the apoptosis is a significant event during fracture repair. There is concern that the TUNEL method might have slightly overestimated the true number of apoptotic cells on decalcified bone paraffin sections because of decalcification, paraffin embedding, and sectioning causing false labeling. In this study, we have used paraffin-embedded nerve tissue as a negative control for the TUNEL staining and found no or minimal staining, as we expected. In a methodological control, we treated the nerve tissue with DNAse I to break the DNAs, and we found extensive

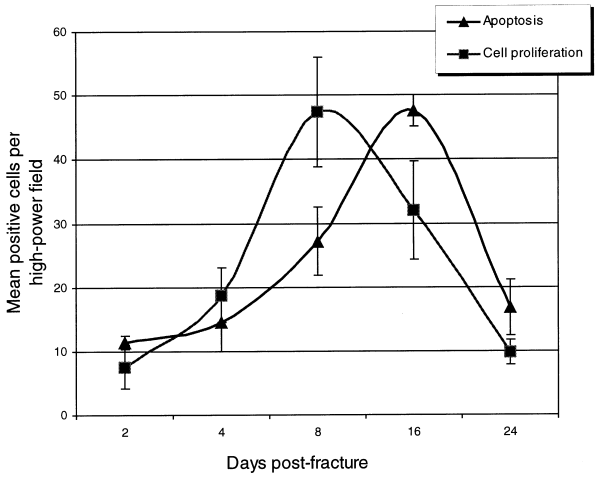

FIG. 4. Plot showing comparison of cell proliferation and apoptosis during fracture healing (days 2–24). Mean PCNA and TUNEL positively labeled cells per high-power field and SEs at different time points were plotted. Cell proliferation peaked on day 8 ($p < 0.05$, compared with the rest of the time points, Student's *t*-test), and significantly declined on day 16 and day 24, respectively. The number of TUNEL-labeled cells significantly increased on day 8 ($p < 0.05$, Student's *t*-test, compared with day 2 and day 4), peaked on day 16 ($p < 0.05$, compared with the rest of the time points, Student's *t*-test), and declined significantly ($p < 0.05$, Student's *t*-test) on day 24 postfracture.

TUNEL labeling. These data suggest that the TUNEL method used in this study was applied properly. Although we cannot completely rule out the possibilities of artifacts on TUNEL staining, one would expect the artifacts (if any) would apply to all the tissues examined, creating a background level that would not prevent comparisons over time. Therefore, the numbers of PCNA- or TUNEL-positive cells are only relative representatives of the true numbers of cell proliferation and apoptosis in the tissues studied in this experimental system and cannot be used as a true estimate or comparison with other systems.

The appearance of empty lacunae within the bone near the line of fracture and positive TUNEL labeling (Figs. 2C and 2I) are in accord with previous findings, indicating programmed cell death of osteocytes.[35] Noble et al.[35] first described the apoptotic changes in lacunae osteocytes in rapidly modeling and remodeling bone. TUNEL labeling was minimal during the initial rise and peak of cell proliferation (days 2–8), indicating little apoptosis during the early phases of repair, which was confirmed by the continuous rise of the total callus area during this period (Fig. 1). Apoptotic cell death increased during the later stages of repair and peaked at day 16 postfracture (Table 1 and Fig. 4), at which point the total callus area reached its peak and started to drop, suggesting that apoptosis is present in tissues that exhibit enhanced cellular proliferation and remodeling.[36] Therefore, apoptosis may play an important role in initiating callus remodeling during fracture healing. The current findings correlate with Lee et al.[8] who concluded that apoptotic cell death sharply increases as the fracture heals. A significant increase in number of TUNEL-labeled cells was found together with a significant decrease in PCNA-positive cells on day 16 postfracture, indicating that apoptosis counterbalances the mass increase of newly formed gap tissue necessary to unite the fracture ends. Callus remodeling was active on day 16 postfracture, resulting in a fall of the total callus area on day 24 postfracture. In a study of the developing adrenal cortex, Wyllie[13] highlighted apoptosis as being active in balancing most of the mitotic cells. However, the upsurge of apoptosis after cell proliferation was short-lived, decreasing sharply on day 24 postfracture. The peak of apoptotic cell death (day 16) after the peak of cell proliferation (day 8) is possibly a result of the potential osteogenetic cells that invade the fracture site exceeding the number necessary for repair, and, thus, apoptosis functions to eliminate superfluous cells and triggers the callus remodeling process.

Such observations raise the further question of whether the increased levels of apoptosis are associated with fracture healing especially callus remodeling or merely with the increased level of cell numbers. In the present study, histomorphometric analysis demonstrated that the total callus area increased to a maximum at day 16, when cell proliferation was over the peak and apoptosis was at its peak. At day 24 postfracture, there was a marked rise in the amount of new bone, as a proportion of the total callus area. Taken together, these data suggest apoptosis play a role in callus remodeling. Apoptosis functions when death is part of an organized tissue reaction as in embryogenesis,[37] tissue metamorphosis,[38] and organogenesis.[39,40] Apoptosis does not cause an inflammatory response and does not damage adjacent cells, thus proving to be an appropriate mechanism to eliminate cells at the fracture site without damage to remaining cells.[34] The occurrence of apoptosis following cell proliferation at the fracture site supports the view that apoptosis serves as a mechanism not only for controlling cell numbers but also eliminating nonfunctional cells and initiating callus remodeling. Removal of nonfunctional cell types by apoptosis has been shown to prevent the development of defective organisms,[40] thus apoptotic cell death participating during fracture healing may ensure complete and unflawed union of the fracture ends. The dynamic occurrence and disappearance of a mixture of fibrous tissue, cartilage, woven bone and different degrees of tissue or bone remodeling during fracture healing, explains the heterogeneous distribution of the PCNA and TUNEL labeling in the different regions of the fracture callus at different time points.

Recent studies[14,41–43] have provided evidence that signaling systems, genetic determination, and common effector pathways driven by specific proteases are shared by cell proliferation and cell death.[44] The reliance on certain signals emphasizes the existence of a high turnover state in which cell proliferation and cell death are likely to coexist, with their relative quantities being determined by the surrounding microenvironment. The inflammatory milieu at the fracture site may be deprived of conditions necessary to ensure cell survival in the regenerating tissue. The critical choice for cells depends on additional considerations such as the availability of growth factors and local mechanical environment.[36] The striking concurrence of cell prolifera-

TABLE 1. SUMMARY OF CELL PROLIFERATION AND APOPTOSIS AFTER FRACTURE

Days after fracture	*Cell proliferation labeling*			*Apoptosis labeling*		
	Connective tissue	*Cartilage*	*Callus*	*Connective tissue*	*Cartilage*	*Callus*
Day 2	++	N/A	N/A	+	N/A	N/A
Day 4	++	N/A	++	+	N/A	+
Day 8	+++	+++	+++	++	+	++
Day 16	N/A	++	++	N/A	+++	+++
Day 24	N/A	+	+	N/A	+	+

N/A, Not applicable; +, present; ++, strong; +++, very strong.

tion and cell death throughout fracture healing in this study gives credibility to this view. Further knowledge on the availability of certain cell types at a line of fracture and their coordinated removal by apoptosis could result in better prognosis of bone healing and provide a better insight to bone disorders and disease states.

In conclusion, it is evident from this study that cell proliferation and apoptosis, despite being two opposing processes, are coupled events of fracture repair. The results suggest that the occurrence of cell proliferation and apoptosis probably is under the influence of a common effector pathway. An understanding of the cellular events and of the molecular pathways that govern the events during fracture healing is important to the future advancement of fracture treatment.

ACKNOWLEDGMENTS

This study was funded in part by a grant from The British Orthopaedic Association Wishbone Trust (project grant 282).

REFERENCES

1. Bruder SP, Fink DJ, Caplan AI 1994 Mesenchymal stem cells in bone development bone repair and skeletal regeneration therapy. J Cell Biochem **56:**283–294.
2. Jacobson D, Weil M, Raff MC 1997 Programmed cell death in animal development. Cell **88:**347–354.
3. Ferguson C, Aplern E, Miclau T, Helms J 1999 Does adult fracture repair recapitulate embryonic skeletal formation? Mech Dev **87:**57–66.
4. Vortkamp A, Pathi S, Peretti GM, Caruso EM, Zaleske DJ, Tabin CJ 1998 Recapitulation of signals regulating embryonic bone formation during postnatal growth and in fracture repair. Mech Dev **71:**65–76.
5. Sandberg MM, Aro HT, Vuorio EI 1993 Gene expression during bone resorption. Clin Orthop **89:**292–312.
6. Manolagas SC 2000 Birth and death of bone cells: Basic regulatory mechanisms and implications for the pathogenesis and treatment of osteoporosis. Endocr Rev **21:**115–137.
7. Iwaki A, Jingushi S, Oda Y, Izumi T, Shida JI, Tsuneyoshi M, Sugioka Y 1997 Localization and quantification of proliferating cells during rat fracture repair: Detection of proliferating cell nuclear antigen by immunohistochemistry. J Bone Miner Res **12:**96–102.
8. Lee FY, Choi YN, Beherns FF, Defoun DO, Einhorn TA 1998 Programmed removal of chondrocytes during endochondral fracture healing. J Orthop Res **16:**144–150.
9. McKibbin B 1978 The biology of fracture healing in long bones. J Bone Joint Surg Br **60:**150–162.
10. Einhorn TA 1998 The cell and molecular biology of fracture dealing. Clin Orthop **355**(Suppl):S7–S21.
11. Aizawa T, Kokubun S, Tanaka Y 1997 Apoptosis and proliferation of growth plate chondrocytes in rabbits. J Bone Miner Res **79:**483–486.
12. O'Connor L, Huang DC, O'Reilly LA, Strasser A 2000 Apoptosis and cell division. Curr Opin Cell Biol **12:**257–263.
13. Wyllie AH 1995 Death from inside out: An overview. In: Dexter TM, Raff MC, Wyllie AH (eds.) The Role of Apoptosis in Development Tissue Homeostasis and Malignancy. The Royal Society, Champan and Hall, London, UK, pp. 1–5.
14. Joyce ME, Jingushi S, Bolander ME 1990 TGF-β in the regulation of fracture repair. Orthop Clin North Am **21:**199–209.
15. Einhorn TA, Majeskan RJ, Rush EB, Levine PM, Horowitz MC 1995 The expression of cytokine activity by fracture callus. J Bone Miner Res **10:**1272–1281.
16. Guo M, Hay BA 1999 Cell proliferation and apoptosis. Curr Opin Cell Biol **11:**745–752.
17. Wyllie AH, Kerr JFR, Currie AR 1980 Cell Death: The significance of apoptosis. Int Rev Cytol **68:**251–306.
18. Kroemer G, Petie P, Zamzami N, Lvayssiere J, Mignotte B 1995 The biochemistry of programmed cell death. FASEB J **9:**1277–1287.
19. Landry PS, Sadasiven K, Marino A, Albright JA 1997 Apoptosis in co-coordinated regulation with osteoblasts formation during bone healing. Tissue Cell **29:**413–419.
20. Jilka RL, Weinstein RS, Bellido T, Parfitt AM, Manolagas SC 1998 Osteoblast programmed cell death (Apoptosis): Modulation by growth factors and cytokines. J Bone Miner Res **13:**793–803.
21. Lynch MP, Capparelli C, Stein JL, Stein GS, Lian JB 1998 Apoptosis during bone-like tissue development in vitro. J Cell Bioch **68:**31–49.
22. Hughes DE, Boyce BF 1997 Apoptosis in bone physiology and disease. Mol Pathol **50:**132–137.
23. Vaux DL, Cory J, Adams JM 1998 Bcl-2 gene promotes haempoptetic cell survival and co-operates with c-myc to immortalise B-cells. Nature **335:**440–442.
24. Strasser A, Huang DCS, Vaux DL 1997 The role of the bcl-2/ced-9 gene family in cancer and general implications of defects in cell death control for tumorigenesis and resistance to chemotherapy. Biochem Biophys Acta **1333:**F151–F178.
25. Olmedo ML, Landry PS, Sadasivan KK, Albright JA, Meer WD, Routh RR, Marino AA 1999 Regulation of osteoblasts levels during bone healing. J Orthop Trauma **13:**356–362.

26. Connolly CK, Li G, Dickson G, Marsh DR 2000 Effects of the COX-2 inhibitor (Meloxicam) on fracture healing. J Bone Miner Res **15:**S1;S343.
27. Modak SP, Bollum FJ 1970 Terminal lens cell differentiation 3 Initiator activity of DNA during nuclear degeneration. Exp Cell Res **62:**421–432.
28. Gavrieli Y, Sherman Y, Ben–Sasson SA 1992 Identification of programmed cell death in situ: A specific labelling of nuclear DNA fragmentation. J Cell Biol **119:**493–501.
29. Fox SE, Leek RD, Weekes MP, Whitehouse RM, Gater KC, Harris AL 1995 Quantitation and prognostic values of breast cancer angiogenesis: Comparison of microvessel density chalky count and computer image analysis. J Pathol **177:**275–283.
30. Li G, Simpson AHRW, Kenwright J, Triffitt JT 1997 Assessment of cell proliferation in regenerating bone during distraction osteogenesis at different distraction rates. J Orthop Res **14:**152–158.
31. Nakahara H, Bruder SP, Haynesworth SE 1990 Bone and cartilage formation in diffusion chambers by sub cultured cells derived from the periosteum. Bone **11:**181–188.
32. Ozaki A, Masaya T, Seijikinoshta J, Saura L 2000 Role of fracture haemtoma and periosteum during fracture healing in rats; Interaction of fracture haematoma and the periosteum in the initial steps of the healing process. J Orthop Sci **5:**64–70.
33. Tonna EA, Cronkite EP 1963 The periosteum Autoradiographic studies on cellular proliferation and transformation utilizing tritiated thymidine. Clin Orthop **30:**218–233.
34. Gibson G 1998 Active role of chondrocyte apoptosis in endochondral ossification. Microsc Res Tech **43:**191–204.
35. Noble BS, Stevens H, Loveridge T, Reeve J 1999 Identification of apoptotic changes in osteocyte in normal and pathological human bone. Bone **20:**273–282.
36. Meyer T, Meryer V, Stratmann V, Weismann HP, Joos V 1999 Identification of apoptotic cell death in distraction osteogenesis. Cell Biol Int **23:**439–446.
37. Schwartzman RA, Cidlowski JA 1993 Apoptosis: The biochemistry and molecular biology of programmed cell death. Endocr Rev **14:**135–151.
38. Walker NI, Bennett RE, Kerr JFR 1989 Cell death by apoptosis during involution of the lactating breast in mice and rats. Am J Anat **185:**19–32.
39. Schweichel JU, Merker HJ 1975 The morphology of various types of cell death in prenatal tissues. Teratology **7:**253–266.
40. Clarke PG, Clarke S 1996 Nineteenth century research on naturally occurring cell death and related phenomena. Anat Embryol (Berl) **193:**81–99.
41. Hughes DE, Wright KR, Mundy GR, Boyce BF 1994 TGFβ1 induces osteoclast apoptosis in vitro. J Bone Miner Res **9:**Sl; S138–145.
42. Hughes DE, Wright KR, Uy HL, Sasaki A, Yoneda T, Roodman GD, Mundy GR, Boyce BF 1995 Bisphosphonate promotes apoptosis in murine osteoclasts in vitro and vivo. J Bone Miner Res **10:**1478–1487.
43. Kamedi T, Mano H, Yuasa T 1997 Eostrogen inhibits bone resorption by directly inducing apoptosis of the bone resorbing osteoclasts. J Exp Med **186:**489–495.
44. Raff MC 1992 Cell Death and survival. Nature **356:**397–398.

Address reprint requests to:
Gang Li, B.Med., D.Phil.
The Department of Trauma and Orthopedic Surgery
Queen's University of Belfast
Musgrave Park Hospital
Stockman's Lane
Belfast BT9 7JB, UK

Received in original form September 27, 2001; in revised form December 12, 2001; accepted December 21, 2001.